

Revision 1

Decagonite, $\text{Al}_{71}\text{Ni}_{24}\text{Fe}_5$, a quasicrystal with decagonal symmetry from the Khatyrka CV3 carbonaceous chondrite

LUCA BINDI^{1*}, NAN YAO², CHANEY LIN³, LINCOLN S. HOLLISTER⁴, CHRISTOPHER L. ANDRONICOS⁵, VADIM V. DISTLER⁶, MICHAEL P. EDDY⁷, ALEXANDER KOSTIN⁸, VALERY KRYACHKO⁶, GLENN J. MACPHERSON⁹, WILLIAM M. STEINHARDT¹⁰, MARINA YUDOVSKAYA⁶ and PAUL J. STEINHARDT^{3,11}

¹Dipartimento di Scienze della Terra, Università di Firenze, Via La Pira 4, I-50121 Florence, Italy

²Princeton Institute for the Science and Technology of Materials, Bowen Hall, Princeton University, Princeton, NJ 08544, USA

³Department of Physics, Princeton University, Jadwin Hall, Princeton, NJ 08544, USA

⁴Department of Geosciences, Princeton University, Guyot Hall, Princeton, NJ 08544, USA

⁵Division of Earth and Atmospheric Sciences, Purdue University, West Lafayette, IN 47907, USA

⁶Institute of Geology of Ore Deposits, Petrography, Mineralogy, and Geochemistry (IGEM), Russian Academy of Sciences, Staromonetny per. 35, Moscow, 119017 Russia

⁷Department of Earth, Atmospheric, and Planetary Sciences, Massachusetts Institute of Technology, Cambridge, MA 02139, USA

⁸Geoscience Technology, BHP Billiton, Houston, TX 77056, USA

⁹Department of Mineral Sciences, National Museum of Natural History, Smithsonian Institution, Washington DC, 20560, USA

¹⁰Department of Earth and Planetary Sciences, Harvard University, 20 Oxford Street, Cambridge, MA 02138, USA

¹¹Princeton Center for Theoretical Science, Princeton University, Princeton, NJ 08544 USA

*E-mail: luca.bindi@unifi.it

ABSTRACT

Decagonite is the second natural quasicrystal, after icosahedrite ($\text{Al}_{63}\text{Cu}_{24}\text{Fe}_{13}$), and the first to exhibit the crystallographically forbidden decagonal symmetry. It was found as rare fragments up to $\sim 60 \mu\text{m}$ across in one of the grains (labeled number 126) of the Khatyrka meteorite, a CV3 carbonaceous chondrite. The meteoritic grain contains evidence of a heterogeneous distribution of pressures and temperatures that occurred during impact shock, in which some portions of the meteorite reached at least 5 GPa and 1200 °C. Decagonite is associated with Al-bearing trevorite, diopside, forsterite, ahrensite, clinoenstatite, nepheline, coesite, pentlandite, Cu-bearing troilite, icosahedrite, khatyrkite, taenite, Al-bearing taenite and steinhardtite. Given the exceedingly small

38 size of decagonite, it was not possible to determine most of the physical properties for the mineral.
39 A mean of 7 electron microprobe analyses (obtained from three different fragments) gave the
40 formula $\text{Al}_{70.2(3)}\text{Ni}_{24.5(4)}\text{Fe}_{5.3(2)}$, on the basis of 100 atoms. A combined TEM and single-crystal X-
41 ray diffraction study revealed the unmistakable signature of a decagonal quasicrystal: a pattern of
42 sharp peaks arranged in straight lines with ten-fold symmetry together with periodic patterns taken
43 perpendicular to the ten-fold direction. For quasicrystals, by definition, the structure is not reducible
44 to a single three-dimensional unit cell, so neither cell parameters nor Z can be given. The likely
45 space group is $P10_5/mmc$, as is the case for synthetic $\text{Al}_{71}\text{Ni}_{24}\text{Fe}_5$. The five strongest powder-
46 diffraction lines [d in Å (I/I_0)] are: 2.024 (100), 3.765 (50), 2.051 (45), 3.405 (40), 1.9799 (40). The
47 new mineral has been approved by the IMA-NMNC Commission (IMA2015–017) and named
48 decagonite for the ten-fold symmetry of its structure. The finding of a second natural quasicrystal
49 informs the longstanding debate about the stability and robustness of quasicrystals among
50 condensed matter physicists and demonstrates that mineralogy can continue to surprise us and have
51 a strong impact on other disciplines.

52 **Keywords:** quasicrystal, aluminum, meteorite, chemical composition, TEM, X-ray diffraction, new
53 mineral, decagonite.

54

55

INTRODUCTION

56 Quasicrystals, solids with quasiperiodic atomic arrangements that violate the mathematical
57 constraints of conventional crystallography, exhibit rotational symmetry forbidden to crystals, such
58 as five-fold, seven-fold and higher-order symmetry axes (Levine and Steinhardt 1984; Shechtman et
59 al. 1984). The first occurrence of a quasicrystalline phase in nature, icosahedrite $\text{Al}_{63}\text{Cu}_{24}\text{Fe}_{13}$
60 (Bindi et al. 2009, 2011), displayed a five-fold symmetry in two dimensions and icosahedral
61 symmetry in three dimensions and was found in the Khatyrka meteorite, a CV3 carbonaceous
62 chondrite (Steinhardt and Bindi 2012; MacPherson et al. 2013; Bindi and Steinhardt 2014). The
63 discovery represents a breakthrough in mineralogy and in condensed matter physics. The intriguing
64 discovery in Grain 126 of the Khatyrka meteorite (Bindi et al. 2014, 2015) of steinhardtite grains
65 with composition $\text{Al}_{0.38-0.50}\text{Ni}_{0.32-0.40}\text{Fe}_{0.10-0.30}$, and the fact that decagonal quasicrystals have been
66 reported in the Al-Ni-Fe system (Tsai et al. 1989), stimulated us to continue the search for other
67 quasicrystals.

68 Here we report the description of the second natural quasicrystal and the first with decagonal
69 symmetry, which is named decagonite for the ten-fold symmetry of its structure. The mineral and
70 its name have been approved by the IMA Commission on New Minerals, Nomenclature and
71 Classification (IMA2015–017). The holotype material is deposited in the mineralogical collections

of the Museo di Storia Naturale, Università di Firenze (Italy), under catalogue number 3146/I.

OCCURRENCE

Decagonite was found in Grain 126, one of the meteoritic fragments (Fig. 1; see Hollister et al. 2014 for more details) found during an expedition to the Koryak Mountains in far eastern Russia in 2011 (Steinhardt and Bindi 2012; Bindi and Steinhardt 2014) as a result of a search for material that would provide information on the origin of icosahedrite (Bindi et al. 2009, 2011, 2012; MacPherson et al. 2013; Hollister et al. 2014).

In the meteoritic fragments, which present a range of evidence indicating that an impact shock generated a heterogeneous distribution of pressures and temperatures in which some portions of the meteorite reached at least 5 GPa and 1200 °C, decagonite occurs as small grains, one of which is in contact with a $(\text{Fe,Mg})_2\text{SiO}_4$ phase (marked “OI” in the bottom panel of Fig. 1). This is either an intermediate composition olivine similar to the Fo_{45-50} found in Grain 125 or the high-pressure polymorph ahrensite, which was also observed in Grain 125 (Hollister et al. 2014). Other minerals identified in the Khatyrka meteorite fragments include trevorite, diopside, forsterite, ahrensite, clinoenstatite, nepheline, coesite, stishovite, pentlandite, Cu-bearing troilite, icosahedrite, khatyrkite, cupalite, taenite, Al-bearing taenite, Ni-Al-Mg-Fe spinels, magnetite, aluminum, steinhardtite and an unnamed spinelloid with composition $\text{Fe}_{3-x}\text{Si}_x\text{O}_4$ ($x \approx 0.4$).

The three identified fragments of decagonite are generally anhedral, up to 60 μm across, and do not contain inclusions or intergrowths of other minerals. Decagonite is metallic, grey to black in color. It is not possible to calculate the density because, as noted below, there does not exist a three-dimensional unit cell or a value of Z for a quasicrystal. Moreover, the density was not measured owing to the very small size of the fragments.

EXPERIMENTAL METHODS

X-ray diffraction

Two decagonite fragments were mounted on two different 0.005 mm diameter carbon fibers (which were, in turn, attached to glass rods) and checked on both a CCD-equipped Oxford Diffraction Xcalibur 3 single-crystal diffractometer, operating with $\text{MoK}\alpha$ radiation ($\lambda = 0.71073 \text{ \AA}$), and an Oxford Diffraction Xcalibur PX Ultra diffractometer equipped with a 165 mm diagonal Onyx CCD detector at 2.5:1 demagnification operating with $\text{CuK}\alpha$ radiation ($\lambda = 1.5406 \text{ \AA}$). One of the fragments consisted of many tiny grains and thus a powder diffraction pattern was collected (Table 1). The pattern matched precisely that reported for the synthetic decagonal $\text{Al}_{71}\text{Ni}_{24}\text{Fe}_5$ quasicrystal (Tsai et al. 1989). The diffraction analysis of a second fragment revealed the

107 unmistakable signature of a decagonal quasicrystal: a pattern of sharp peaks arranged in straight
108 lines with ten-fold symmetry together with periodic patterns taken perpendicular to the ten-fold
109 direction (as illustrated in Fig. 2). The likely space group of decagonite is $P10_5/mmc$, as is the case
110 for synthetic $Al_{71}Ni_{24}Fe_5$ (Tsai et al. 1989).

111 **Chemical analyses**

112 Three decagonite fragments were analyzed via wavelength dispersive spectroscopy (WDS)
113 using a JEOL JXA-8600 electron microprobe at 15 kV, 20 nA beam current, and 1 μm beam
114 diameter. Variable counting times were used: 30 s for Al, Ni and Fe, and 60 s for the minor
115 elements Mg, Si, Cr, P, Co, Cu, Cl, Ca, Zn, and S. Replicate analyses of synthetic $Al_{53}Ni_{42}Fe_5$ were
116 used to check accuracy and precision. The crystal fragments were found to be homogeneous within
117 analytical error. The standards used were: Al metal, synthetic Ni_3P (Ni, P), synthetic FeS (Fe), Mg
118 metal, Si metal, Cr metal, Co metal, Cu metal, synthetic $CaCl_2$ (Ca, Cl) and synthetic ZnS (Zn, S).
119 Magnesium, Si, Cr, P, Co, Cu, Cl, Ca, Zn, and S were found to be equal to or below the limit of
120 detection (0.01 wt%).

121 Seven point analyses on different spots were performed on the three samples. Table 2 reports
122 the chemical analyses (in wt% of elements), standard deviations, and atomic ratios calculated on
123 100 atoms per formula unit.

124 **Transmission electron microscopy**

125 Because of the small size of the grains, the single-crystal X-ray investigation was combined
126 with a structural study done by transmission electron microscopy. The Philips CM200-FEG TEM
127 was operated at 200 KeV with an electron beam size ranging from 30 nm to 0.2 μm . The sample
128 was placed on a Cu mesh TEM grid (300 mesh, 3mm in diameter) that was previously covered by a
129 thin carbon layer (support film). Energy Dispersive (EDS) data were obtained using Evex
130 NanoAnalysis System IV attached to the Philips CM200-FEG TEM. A small probe diameter of 20-
131 100 nm was used, with a count rate of 100-300 cps and an average collection time of 180 s. The
132 quantitative analyses were taken at 200 kV and are based on using pure elements and the NIST
133 2063a standard sample as a reference under the identical TEM operating conditions.

134

135

RESULTS AND DISCUSSION

136 The TEM study of one of the three studied fragments of decagonite revealed that, at the sub-
137 micron length scale, the particles are homogeneous. Selected area electron diffraction patterns (Fig.
138 3) consist of sharp peaks arranged either in a lattice with ten-fold symmetry and periodic patterns
139 perpendicular to the ten-fold direction. This pattern is characteristic of a decagonal quasicrystal.
140 The high-resolution transmission electron microscopy image in Figure 3 shows that the real space

141 structure consists of a homogeneous, quasiperiodic and ten-fold symmetric pattern. Collectively,
142 TEM (Fig. 3) and single-crystal X-ray data (Fig. 2) provide conclusive evidence of
143 crystallographically forbidden decagonal symmetry in a naturally occurring phase.

144 As already observed for icosahedrite (Bindi et al. 2009, 2011), decagonite exhibits a high
145 degree of structural perfection, particularly the absence of significant phason strains (Levine et al.
146 1985; Lubensky et al. 1986). This is unusual because this high degree of perfection occurs in a
147 quasicrystal intergrown with other phases under conditions far from equilibrium, and not under
148 controlled laboratory conditions. We think that either the mineral samples formed without phason
149 strain in the first place, or subsequent annealing was sufficient for phason strains to relax away.

150 Figure 4 is a ternary diagram showing the compositions (WDS and EDS data) of all the
151 AlNiFe fragments we analyzed from Grain 126, plotted in terms of atomic percent Al–Ni–Fe. The
152 compositions of steinhardtite (red open circles and black open squares) are approximately collinear
153 with decagonite (green open triangles) and taenite (light blue open diamonds). This suggests a
154 reaction relation amongst these phases. That is, steinhardtite could break down to decagonite and
155 taenite, or taenite plus decagonite could react to produce steinhardtite.

156 The Al–Ni–Fe of the projected composition of the Al-bearing trevorite spinel plots very close
157 to that of steinhardtite in Figure 4. As documented by Hollister et al. (2015), shock can reduce iron,
158 with the oxygen going into the vapor. Similarly, steinhardtite could form as a result of shock of pre-
159 existing Al-bearing trevorite.

160

161

IMPLICATIONS

162 The discovery of two different types of quasicrystals in a meteorite has implications for other
163 scientific disciplines. From the perspective of condensed matter physics, the fact that these phases
164 formed under astrophysical conditions constitutes significant new support for the original proposal
165 (Levine and Steinhardt 1984) that quasicrystals can be energetically stable states of matter, on the
166 same footing as crystals. The fact that both icosahedrite and decagonite contain metallic aluminum
167 represents a challenge to geochemistry, given the strong affinity of Al for oxygen.

168 Conceivably, the Al–Ni–Fe phases might have also formed in the highly reducing conditions
169 near the core-mantle boundary, as we speculated during the early stages of our investigation
170 (Steinhardt and Bindi 2012). This opportunity seems worthy of exploring since it may give us new
171 insights on core composition and properties. However, the origin of the occurrence of Cu with the
172 Al compounds remains elusive.

173 Finally, our discoveries should motivate the re-examination of other terrestrial and
174 extraterrestrial minerals in search of different quasicrystals. We believe that mineralogy can
175 continue to surprise us and have an impact on other disciplines, including cosmochemistry,

176 condensed matter physics, and materials engineering.

177

178

ACKNOWLEDGMENTS

179

180

181

182

183

184

185

186

187

REFERENCES CITED

188

189

190

191

192

193

194

195

196

197

198

199

200

201

202

203

204

205

206

207

208

- Bindi, L., Eiler, J., Guan, Y., Hollister, L.S., MacPherson, G.J., Steinhardt, P.J., and Yao, N. (2012) Evidence for the extra-terrestrial origin of a natural quasicrystal. *Proceedings of the US National Academy of Sciences*, 109, 1396-1401.
- Bindi, L., and Steinhardt, P.J. (2014) The quest for forbidden crystals. *Mineralogical Magazine*, 78, 467-482.
- Bindi, L., Steinhardt, P.J., Yao, N., and Lu, P.J. (2009) Natural Quasicrystals. *Science*, 324, 1306-1309.
- Bindi, L., Steinhardt, P.J., Yao, N., and Lu, P.J. (2011) Icosahedrite, $Al_{63}Cu_{24}Fe_{13}$, the first natural quasicrystal. *American Mineralogist*, 96, 928-931.
- Bindi, L., Yao, N., Lin, C., Hollister, L.S., Andronicos, C.L., Distler, V.V., Eddy, M.P., Kostin, A., Kryachko, V., MacPherson, G.J., Steinhardt, W.M., Yudovskaya, M., and Steinhardt, P.J. (2015) Natural quasicrystal with decagonal symmetry. *Scientific Reports*, 5, 9111.
- Bindi, L., Yao, N., Lin, C., Hollister, L.S., Poirier, G.R., Andronicos, C.L., MacPherson, G.J., Distler, V.V., Eddy, M.P., Kostin, A., Kryachko, V., Steinhardt, W.M., and Yudovskaya, M. (2014) Steinhardtite, a new body-centered-cubic allotropic form of aluminum from the Khatyrka CV3 carbonaceous chondrite. *American Mineralogist*, 99, 2433-2436.
- Hollister, L.S., Bindi, L., Yao, N., Poirier, G.R., Andronicos, C.L., MacPherson, G.J., Lin, C., Distler, V.V., Eddy, M.P., Kostin, A., Kryachko, V., Steinhardt, W.M., Yudovskaya, M., Eiler, J.M., Guan, Y., Clarke, J.J., and Steinhardt, P.J. (2014) Impact-induced shock and the formation of natural quasicrystals in the early solar system. *Nature Communications*, 5:3040 doi:10.1038/ncomms5040.

- 209 Hollister, L.S., MacPherson, G.J., Bindi, L., Lin, C., Guan, Y., Yao, N., Eiler, J.M., and
210 Steinhardt, P.J. (2015) Redox reactions between Cu-Al metal and silicates in the Khatyrka
211 meteorite. 46th Lunar and Planetary Science Conference, 1832, 2394.
- 212 Levine, D., and Steinhardt, P.J. (1984) Quasicrystals: a new class of ordered structures. *Physical*
213 *Review Letters*, 53, 2477-2480.
- 214 Levine, D., Lubensky, T.C., Ostlund, S., Ramaswamy, A., and Steinhardt, P.J. (1985) Elasticity and
215 defects in pentagonal and icosahedral quasicrystals. *Physical Review Letters*, 54, 1520-1523.
- 216 Lubensky, T.C., Socolar, J.E.S., Steinhardt, P.J., Bancel, P.A., and Heiney, P.A. (1986) Distortion
217 and peak broadening in quasicrystal diffraction patterns. *Physical Review Letters*, 57, 1440-
218 1443.
- 219 MacPherson, G.J., Andronicos, C.L., Bindi, L., Distler, V.V., Eddy, M.P., Eiler, J.M., Guan, Y.,
220 Hollister, L.S., Kostin, A., Kryachko, V., Steinhardt, W.M., Yudovskaya, M., and Steinhardt,
221 P.J. (2013) Khatyrka, a new CV3 find from the Koryak Mountains, Eastern Russia. *Meteoritics*
222 *and Planetary Science*, 48, 1499-1514.
- 223 Shechtman, D., Blech, I., Gratias, D., and Cahn J.W. (1984) Metallic phase with long-range
224 orientational order and no translational symmetry. *Physical Review Letters*, 53, 1951-1953.
- 225 Steinhardt, P.J., and Bindi, L. (2012) In search of natural quasicrystals. *Reports on Progress in*
226 *Physics*, 75, 092601-092611.
- 227 Tsai, A.P., Inoue, A., and Masumoto, T. (1989) New decagonal Al-Ni-Fe and Al-Ni-Co alloys
228 prepared by liquid quenching. *Materials Transactions JIM*, 30,150-154.
- 229
230
231
232
233
234
235
236
237
238
239
240
241
242
243
244
245
246
247

FIGURE CAPTIONS

248
249
250
251
252
253
254
255
256
257
258
259
260
261
262
263
264
265
266
267
268
269
270
271
272
273
274
275
276
277
278
279
280
281

Figure 1. The **top panel** shows micro CT-SCAN 3D-images (at different rotations) of the whole Grain 126. The brighter and the darker regions are Cu-Al metals and meteoritic silicates, respectively. The **bottom panel** shows a SEM-BSE image of decagonite (DEC) in apparent growth contact with “olivine” (“OL”). See text for discussion of the “olivine” composition. The image also contains sodalite (SOD).

Figure 2. Reconstructed precession images along the ten-fold symmetry axis (**a**) and perpendicular to the ten-fold direction (**b, c**) obtained using the collected single-crystal X-ray data set (MoK α radiation) from decagonite.

Figure 3. The **top panel** is a high-resolution transmission electron microscopy (HRTEM) image showing that the real space structure of decagonite consists of a homogeneous, quasiperiodic and ten-fold symmetric pattern. The **bottom panel** reports two selected area electron diffraction patterns collected down the ten-fold axis (**left**) and along an axis out of the ten-fold plane (**right**). The combination of quasiperiodicity (ten-fold symmetry) in one plane and periodicity along the third dimension is characteristic of decagonal symmetry.

FIGURE 4. Ternary Al-Ni-Fe diagram reporting all the chemical data we obtained on minerals belonging to Grain 126. The cloud of data in the steinhardtite region (blue downward triangles) lies between decagonite and FeNi solid solution.

TABLE 1. Measured X-ray powder-diffraction data for decagonite (CuK α radiation).

| 2θ ($^\circ$) | d (\AA) | I_{rel} |
|------------------------|----------------------|------------------|
| 23.61 | 3.765 | 50 |
| 26.15 | 3.405 | 40 |
| 38.58 | 2.332 | 25 |
| 44.12 | 2.051 | 45 |
| 44.75 | 2.024 | 100 |
| 45.79 | 1.9799 | 40 |
| 50.63 | 1.8014 | 30 |
| 65.60 | 1.4219 | 35 |
| 78.03 | 1.2235 | 25 |

TABLE 2. Electron microprobe analyses (values and standard deviations in wt% of elements) and atomic ratios (on the basis of 100 atoms) for three fragments of decagonite.

| | 1 | | 2 | | 3 | | | mean |
|-------|-----------|-----------|-----------|-----------|-----------|-----------|-----------|-------|
| | <i>a</i> | <i>b</i> | <i>a</i> | <i>b</i> | <i>a</i> | <i>b</i> | <i>c</i> | |
| Al | 52.23(60) | 51.74(64) | 52.01(71) | 51.60(66) | 52.10(44) | 52.64(40) | 53.01(46) | 52.19 |
| Ni | 39.85(51) | 38.92(49) | 40.45(53) | 39.41(55) | 40.01(34) | 39.23(39) | 39.01(37) | 39.55 |
| Fe | 8.02(10) | 8.74(12) | 7.55(14) | 8.23(15) | 8.10(9) | 8.16(12) | 8.47(11) | 8.18 |
| Total | 100.10 | 99.40 | 100.01 | 99.24 | 100.21 | 100.03 | 100.49 | 99.92 |
| Al | 70.18 | 70.06 | 70.05 | 70.02 | 70.03 | 70.55 | 70.65 | 70.22 |
| Ni | 24.61 | 24.22 | 25.04 | 24.59 | 24.71 | 24.17 | 23.90 | 24.46 |
| Fe | 5.21 | 5.72 | 4.91 | 5.39 | 5.26 | 5.28 | 5.45 | 5.32 |

FIGURE 1

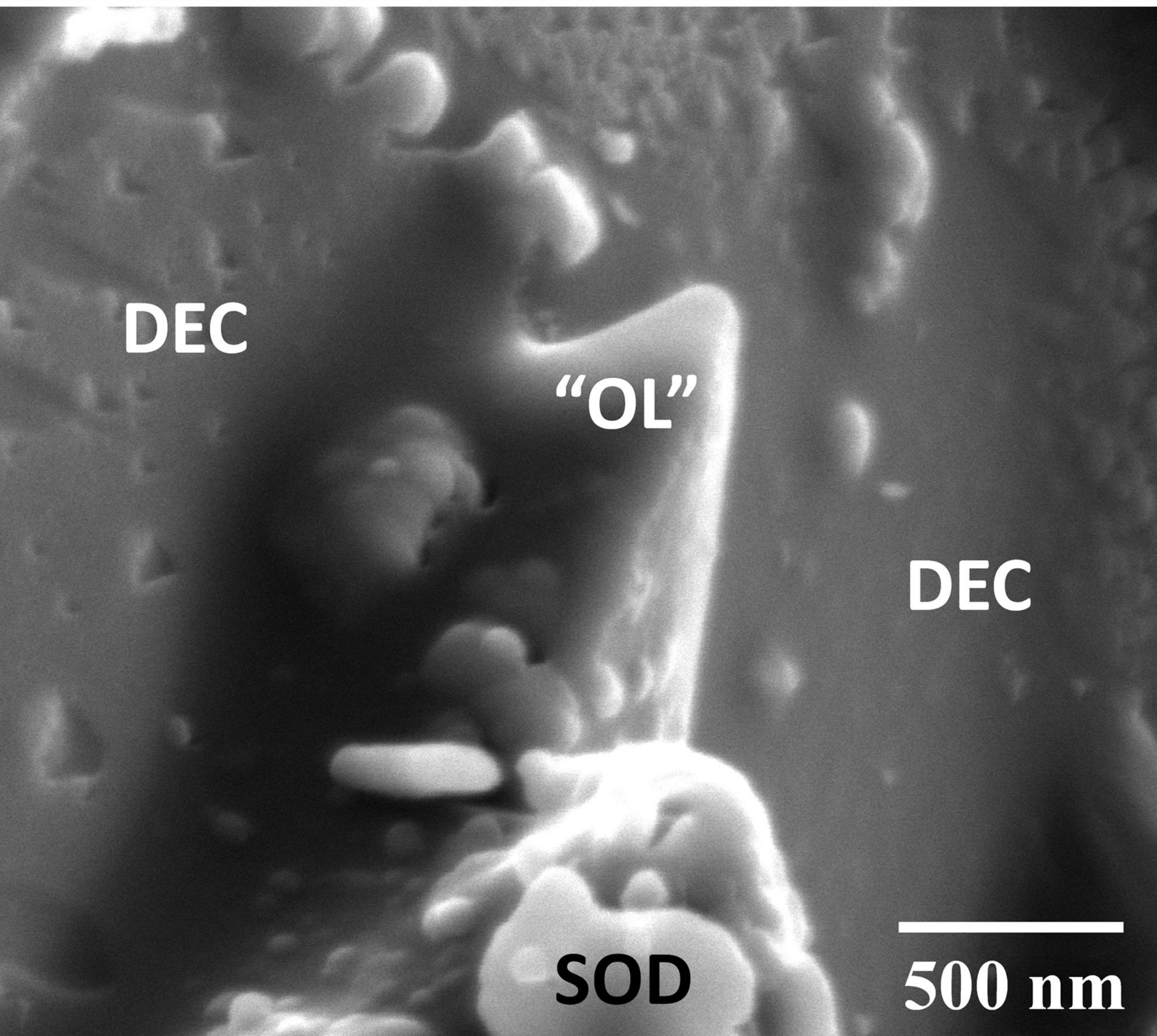
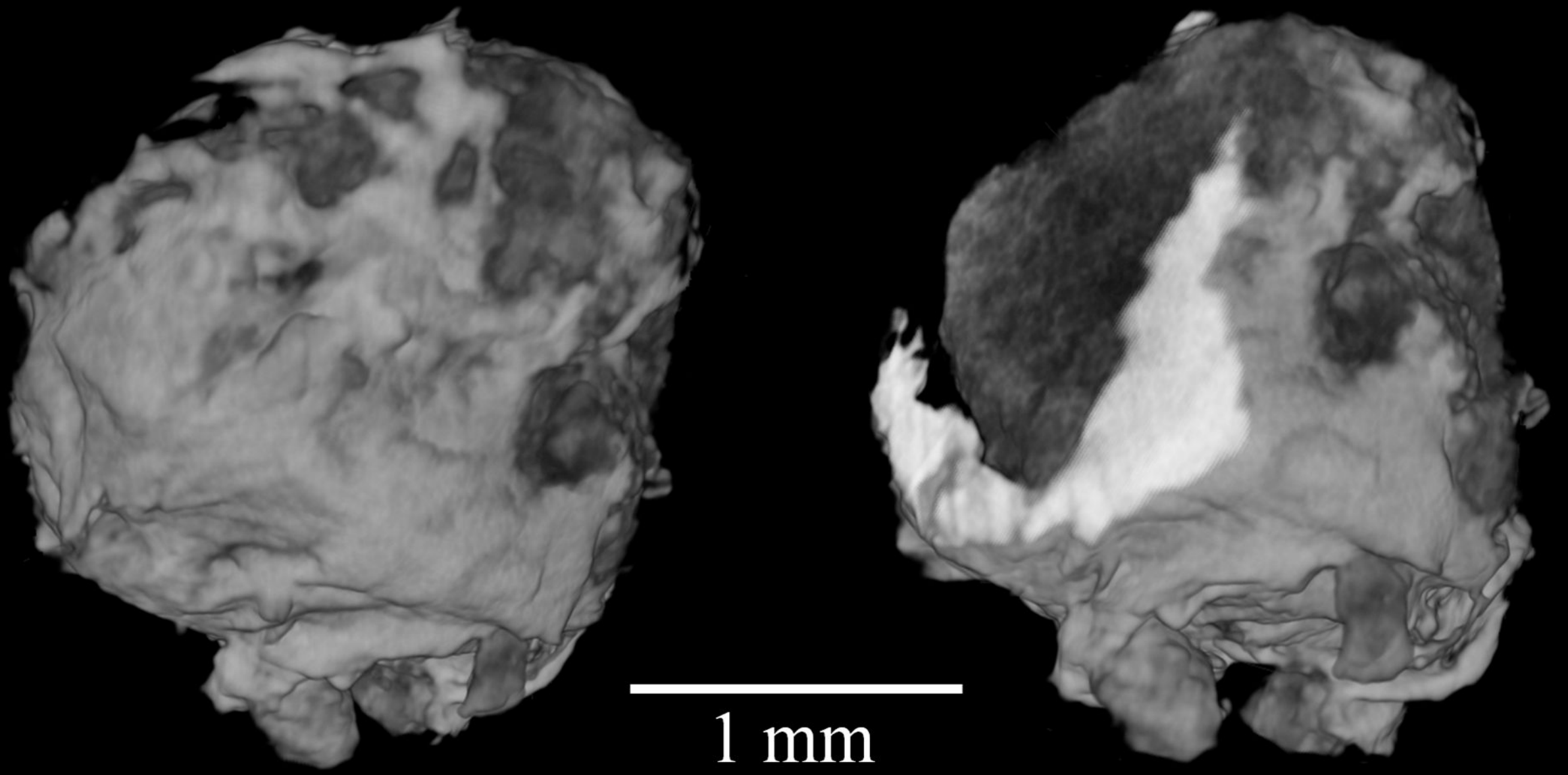


FIGURE 2

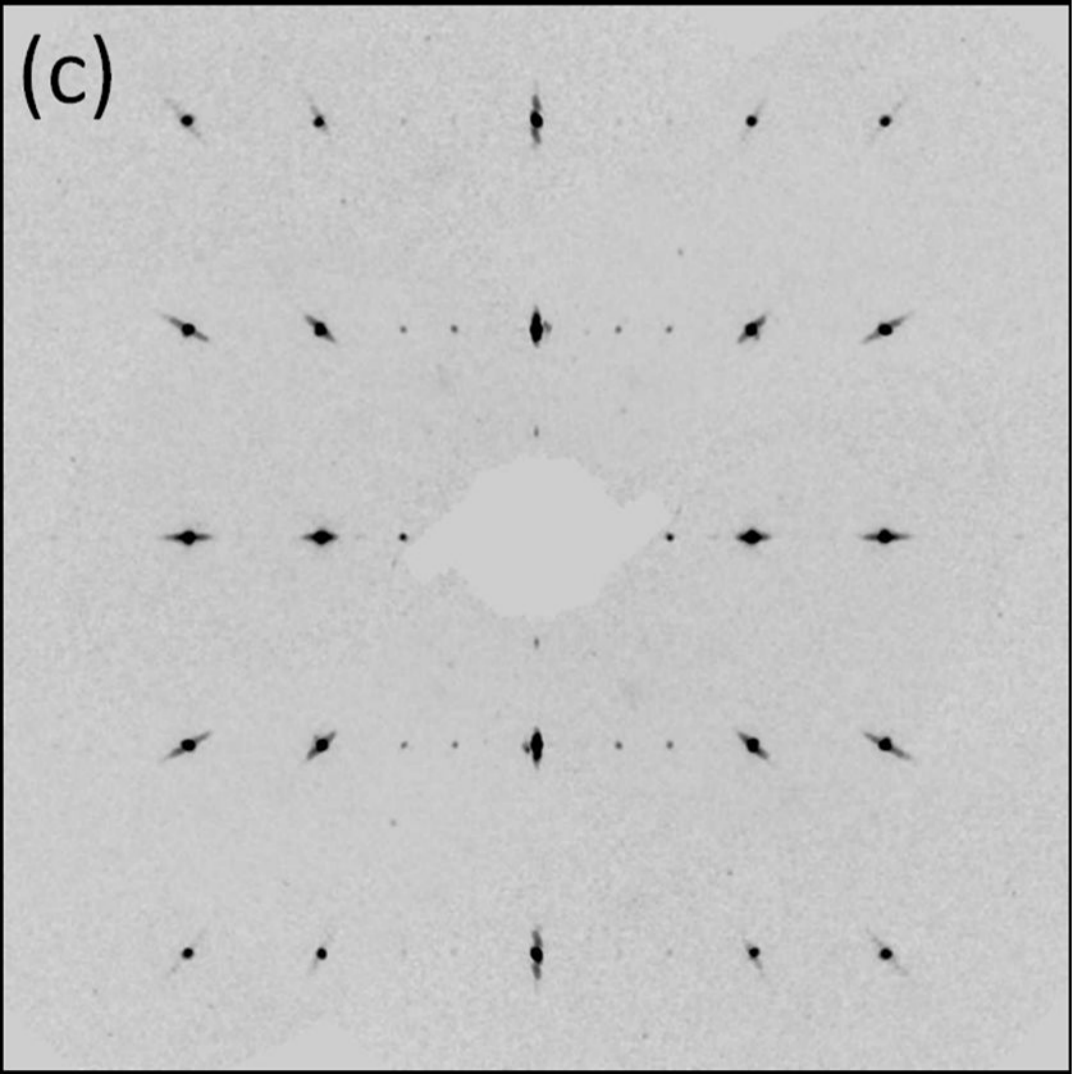
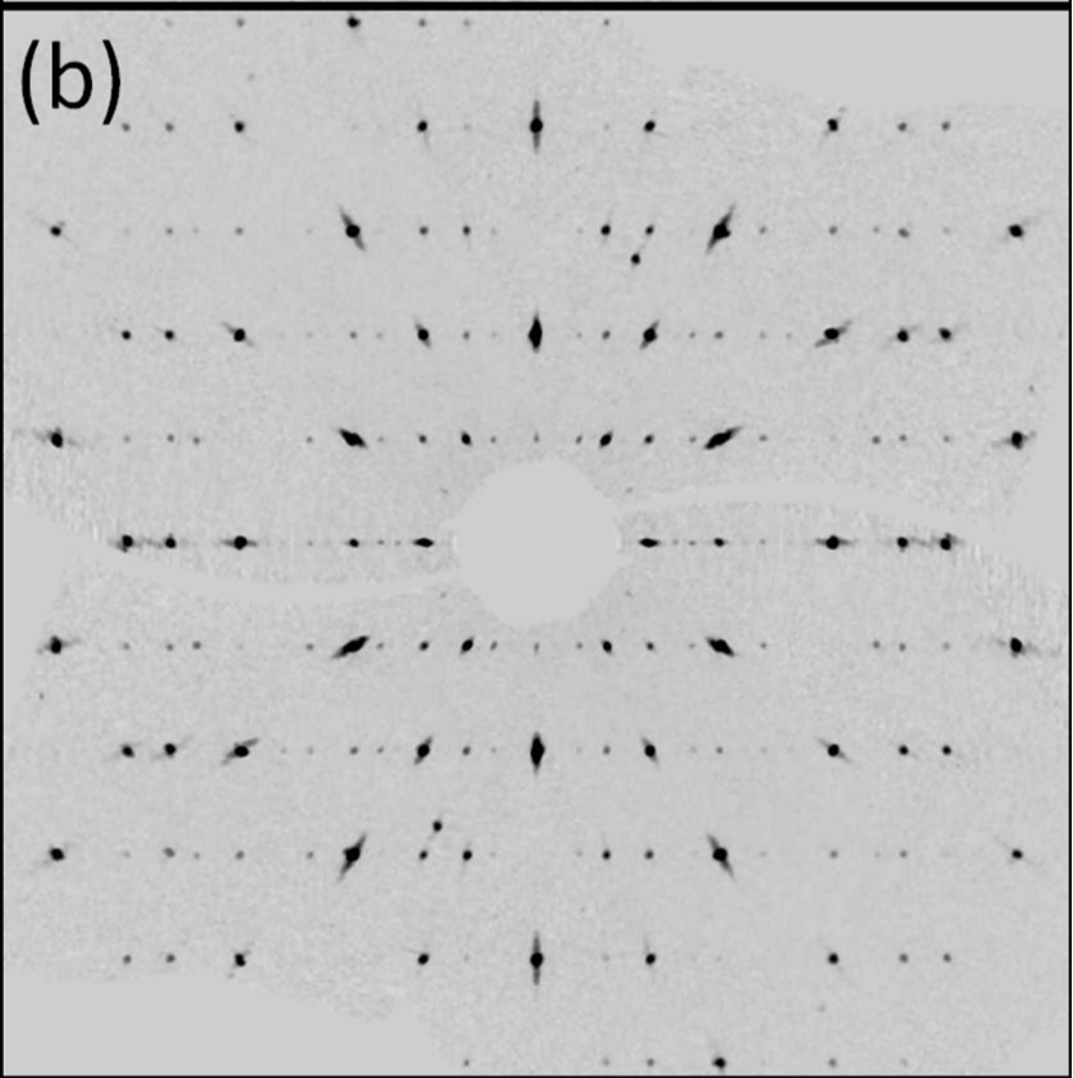
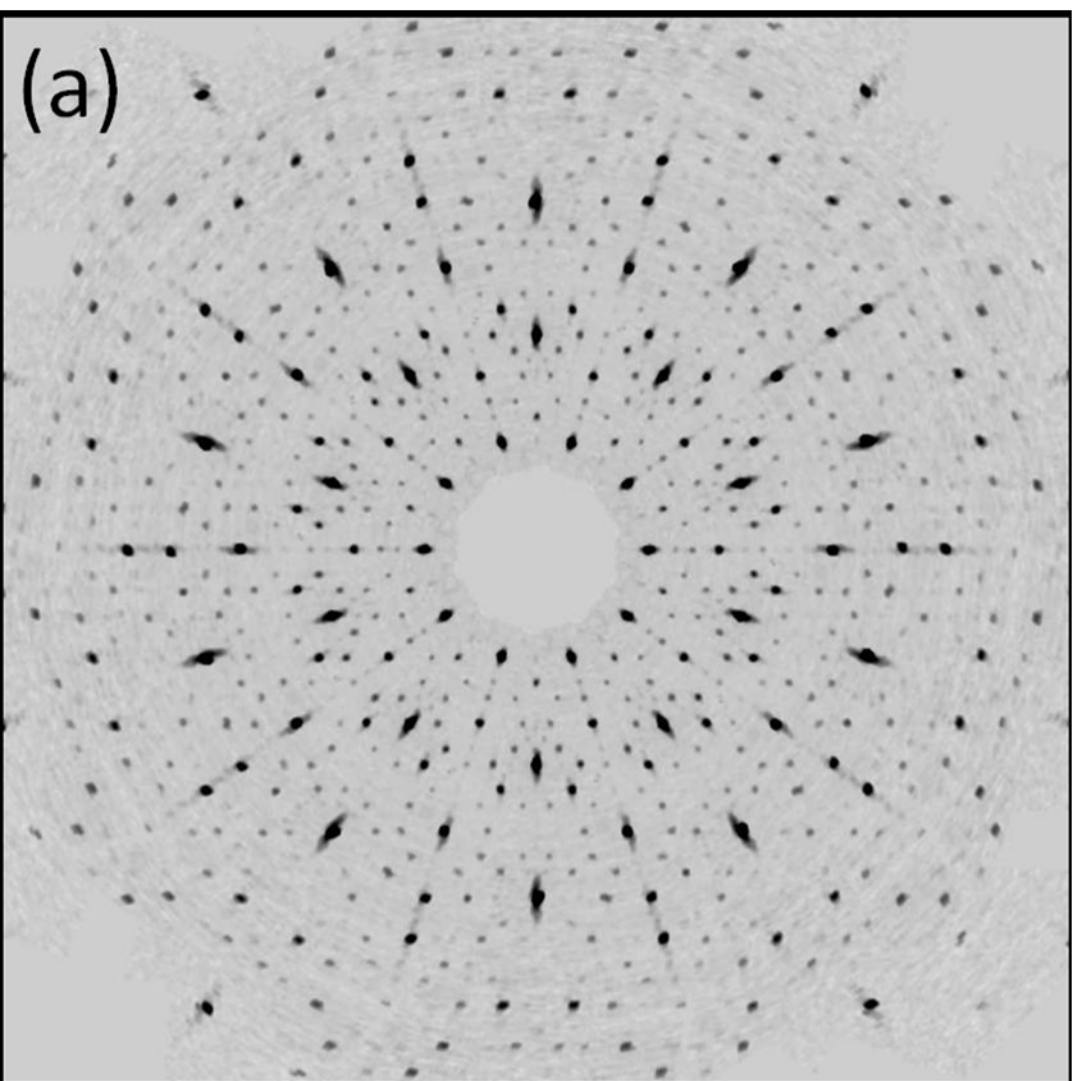


FIGURE 3

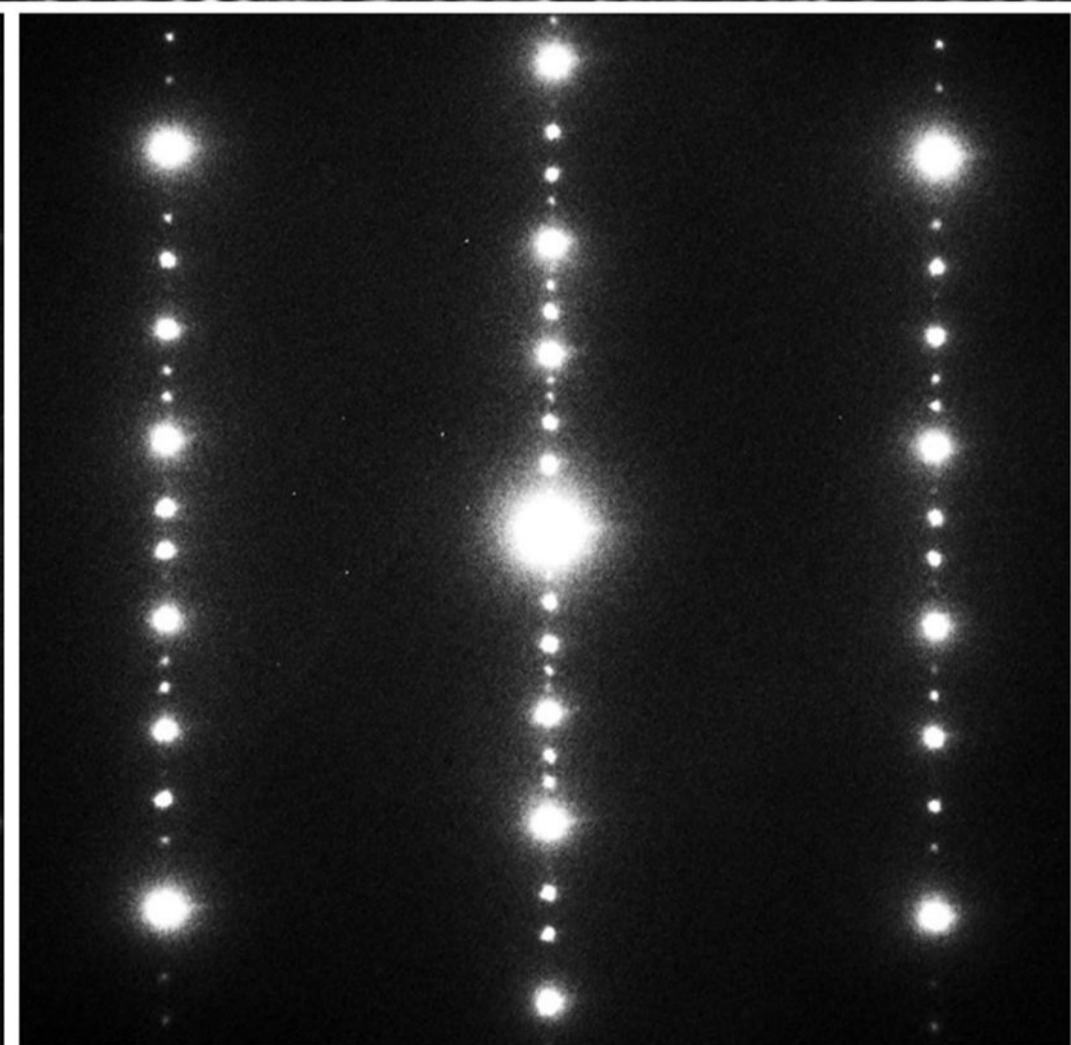
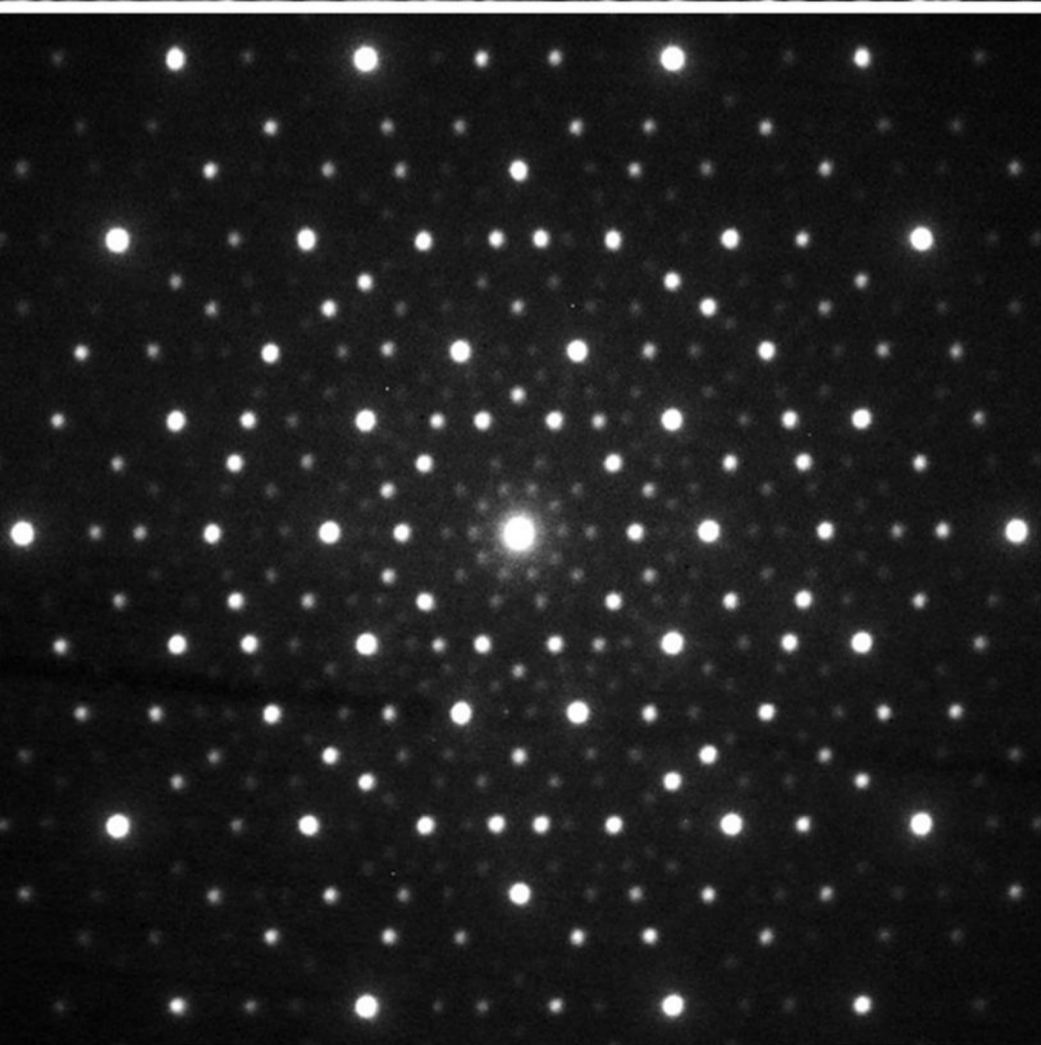
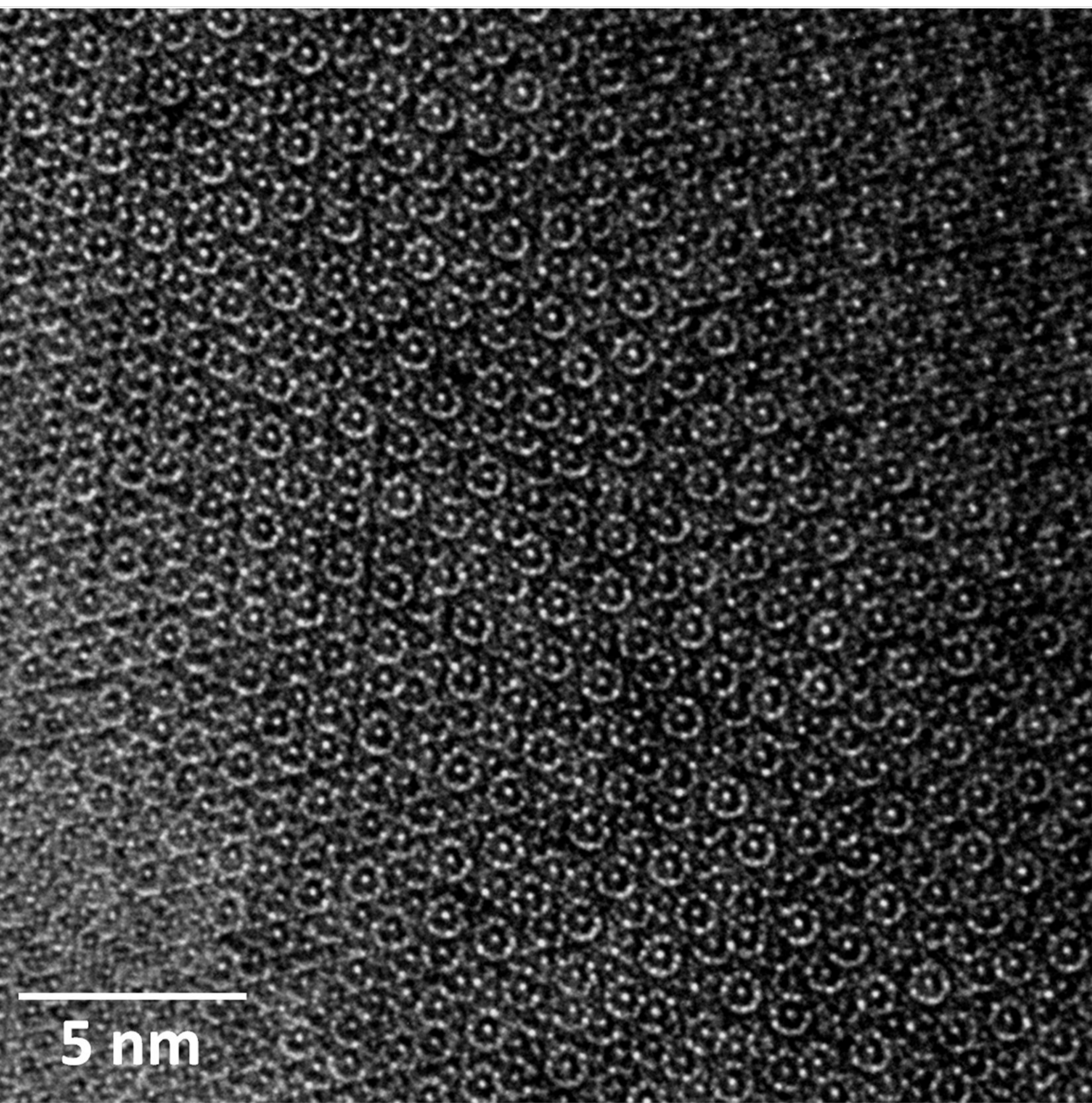


FIGURE 4

